Challenging Glass 6 - Conference on Architectural and Structural Applications of Glass
Louter, Bos, Belis, Veer, Nijsse (Eds.), Delft University of Technology, May 2018.
Copyright © with the authors. All rights reserved.
ISBN 978-94-6366-044-0, https://doi.org/10.7480/cgc.6.2165

Structural Analysis of Slender Glass Panel Subjected to Static and Impact Loading

Marcin Kozłowski [a, b], David Kinsella [a], Kent Persson [a], Jan Kubica [b], Jacek Hulimka [b]
[a] *Faculty of Engineering LTH, Lund University, Lund, Sweden, marcin.kozlowski@construction.lth.se*
[b] *Faculty of Civil Engineering, Silesian University of Technology, Gliwice, Poland*

Slender glass panels are widely used as storefronts and indoor separating walls in shopping malls and public buildings. To ensure that the design and construction is technically safe for general use and that it meets current and accepted technical standards, in-situ testing is required by the building administrator or authorities. A case study was performed of an indoor glass lantern in a public building made from slender two-side supported glass panels with a complex geometry. It provides structural assessments and results of in-situ experiments including static loading and soft body impact test. Results from numerical simulations of impact loading on the glass panels complementing the experimental results are also presented. The in-situ testing proved that the structural design meets current standards regarding the static loading. The soft body impact test proved the safety of the intact panel and the panel with one ply deliberately broken. The numerical study showed that, for a more complicated geometry, the stress distribution can dramatically change over time and that stress concentrations can develop at certain locations at a late stage in the impact history.

Keywords: Glass, Architectural glass, Static loading, Impact loading, In-situ testing, Numerical simulations.

1. Introduction

Slender glass panels are widely used as storefronts and indoor separation walls in shopping malls and public buildings. Whenever glass panels are mounted at identified risk areas, the owner of the building is responsible for ensuring that the design and construction is technically safe for general use and that it meets current and accepted technical standards. This applies especially in the situations when panels are required to ensure protection of neighboring walkways and have to bear the loads of persons leaning against or bumping into the glass.

According to the building standards (EN 1991), the panels should satisfy the basic load requirements such as an internal or external wind load and a static barrier loading with the value depending on the category of the building. The panels should also offer protection to people against cutting and piercing injuries resulting from accidental impact. In identified risk areas, such as the situation where a difference in height constitutes a falling risk, building codes require the use of safety glass, the performance and classification of which is evaluated with the impact pendulum test according to EN 12600. Therefore, the panels are usually made of laminated glass which shows improved post-breakage performance (Delincé et al. 2008, Haldimann 2008). If a single sheet is broken, the interlayer prevents the fragments from being scattered, thus the solution provides a certain level of residual load-bearing capacity and reduces the risk of injury from cuts.

Better knowledge about the performance of unframed, simply supported glass panels under static and dynamic loads is critical regarding its structural behavior in real life conditions. This paper presents a case study of an indoor glass lantern in a public building made from slender glass panels with a large number of ventilation holes. Structural assessment and results of in-situ experiments including static barrier loading and soft body impact test is reported. Results of numerical simulations of the slender glass panels subjected to soft body impact loading complement the experimental results.

2. Case study

The lantern used in the case study was designed as an indoor separating wall supported at the floor and the ceiling. The wall allows natural sunlight to illuminate the stories of the building and is also a part of the ventilation and smoke extraction system in the event of fire. This is reflected in the construction details: a number of holes located in the lower part of the glass panels allows for efficient air flow between the interior floors and the lantern (Fig. 1).

Although the lantern runs through several stories, the glass panels span over two floors and is considered as a separate structure. The glass panels create a glass room with an approximately height of 4.4 m and projection of 15×6 m^2. Each laminated glass panel with the dimensions 0.99×4.38 m^2 consists of two 10 mm thick, clear and fully toughened safety glass sheets with 1.52 mm thick layer of Polyvinyl Butyral (PVB). Near the bottom edge of the panels is an array of 6×6 ventilation holes, each hole being 50 mm in diameter, see Fig. 4a. The space between the holes is 75 mm in both the vertical and horizontal direction. The array of holes starts at about 330 mm above the bottom edge and is located at about 160 mm from the vertical edge. The panels are self-supported along the bottom edge through two nylon setting blocks. Out-of-plane restraints are provided by standard aluminum profiles through rubber gaskets.

According to design documentation, the panels have been designed for several load cases. These included an internal pressure of 0.2 kN/m^2 and a barrier loading of 1.0 kN/m applied at the height of 1.1 m above the floor level. Although the structural design was proven to meet the requirements regarding maximum stress and panel deflection, a decision was made to experimentally verify the panels regarding the load-bearing capacity under static and soft body impact loading. It was decided that two panels of the lantern were designated for in-situ destructive testing after which the elements would be replaced. The following part of the paper presents the set-up of the tests and main results.

2.1. Static loading

The static barrier loading test was performed with respect to the loadings as per EN 1991-1-1. The horizontal loading was applied at the height of 1.1 m above the finished floor level by a hydraulic jack mounted on a steel beam fixed to steel columns located at the corners of the lantern, see Fig. 1a. The stiffness of the steel beam was significantly higher than the glass panel thus it was not affecting the results of the panel's displacement. To ensure that the loading was applied as a linear load, a flat steel bar 15 mm in thickness was bonded to the glass, distributing the load generated by the jack into a line load, see Fig. 1b.

The deflections were measured with a linear variable differential transformer (LDVT) that was installed on the panel approximately 100 mm below the location of the jack. In addition, a set of strain gauges were bonded to the panel at several positions on the tension side of the glass to measure tensile strain. The positions were as follows: one at the level of the steel bar (1), a pair positioned below the load introduction point of the jack (2 and 3) and a pair at the same lever but close to the edges (4 and 5). The strain gauges allowed for the strain distribution in the highest stressed area to be determined and the influence of the holes in the glass on the strain value to be investigated. The locations of the LDVT and the strain gauges are shown in Fig. 1c. The load, displacement and strain in the glass were recorded throughout the entire test with the data acquisition rate of 5 Hz.

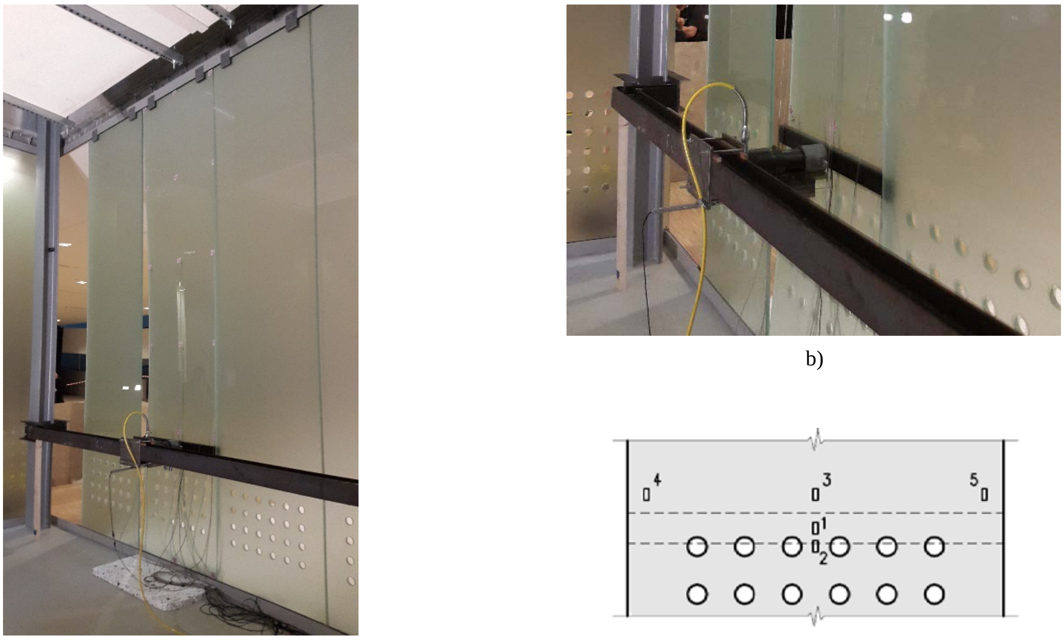

a)

b)

c)

Fig. 1 Static loading test-set up: a) General view, b) Detail of load introduction point, c) Positions of strain gauges and LDVT.

Fig. 2a shows the load versus displacement history obtained from the static test. The test consisted of three main stages. In stage I the loading was ramped up to the value of 1 kN to achieve the level of load required by the standards. This corresponded to a horizontal deflection of 30 mm, which was lower than the maximum allowed as specified by the standards (4380/100=43.8 mm). Then, the deflection was gradually increased by 5 mm up to 50 mm (Stage II) by applying several load levels. Each load level (corresponding to 5 mm increase of the deflection) was followed by 15 minutes of constant load before the load was increased to the next level. In Stage III at the deflection of approximately 50 mm the panel was further loaded up to the limit of the jack's piston (100 mm). At the end of Stage III the load reached the value of 4.4 kN. The tangent stiffness of the panel calculated in stage I was approximately 40% higher compared to the tangent stiffness evaluated from stage III, see Fig. 2a. The decrease in stiffness is mainly caused by stress relaxation of the viscous behavior of the interlayer, which can also be clearly noticed in stage II during the breaks between each increment of load.

Fig. 2b shows tensile stresses calculated from the strain gauges. The stresses were calculated with the Young's modulus of glass of 70 GPa assumed after material product standard EN 572–2:2004. Interesting observations can be made. Firstly, it is clear that the gauge no. 2 shows approximately 40% higher values of stress than at other locations. It can be explained not only by the distance of the sensor to the location of the maximum bending moment but primarily by the influence of holes in the glass resulting in stress concentrations. Secondly, during the 15 minutes breaks in loading within stage II, a clear decrease in stiffness resulting in stress relaxation can be observed. Similar to the decrease in stiffness it can be explained by the viscous properties of the interlayer.

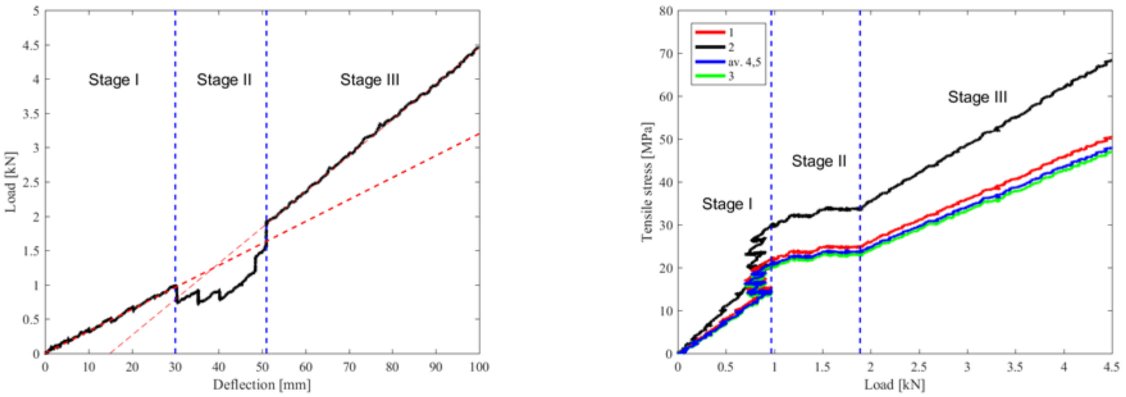

a) b)

Fig. 2 Results of static loading test: a) Load-displacement plot, b) Load-tensile stress (in glass) plots at different locations of strain gauges.

2.2. Soft body impact

Soft body impact test was performed on a panel adjacent to the panel subjected to static linear loading. The principle of the test is presented in Fig. 3a. The impactor used was the pendulum described in EN 12600 with a mass of 50 kg. It consisted of two pneumatic tires inflated with 4 bar air pressure and a steel weight. The impactor was brought to a drop height of 900 mm and released. The panel was hit at three locations: at the center of the set of holes (1), at the center at the height of 1500 mm (2) and close to the edge at the height of 1500 mm (3), see Fig. 3a. Despite considerable deflection of the panel after hits, no breakage of glass occurred. In the next phase, the compressed ply of the laminated glass was deliberately broken using a steel chisel and a hammer. The test was repeated with the drop height reduced to 450 mm. In this case the undamaged ply in the laminate remained intact, see Fig. 3b.

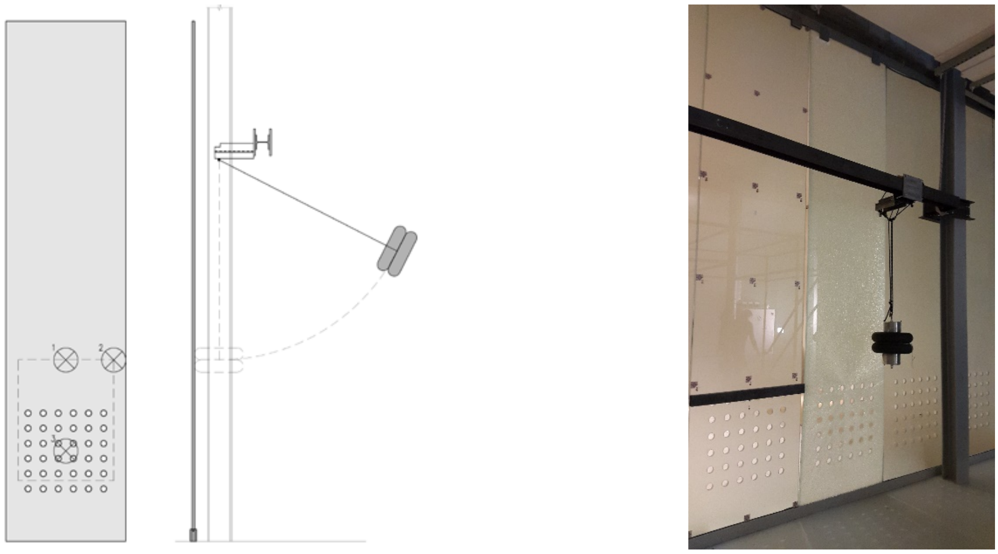

a) b)

Fig. 3 a) Principles of soft body impact loading, b) Laminated glass panel with one ply deliberately broken after impact loading test.

3. Numerical study

A finite element (FE) model was created using the commercial FE program ABAQUS (Simulia 2016) to further study the impact load on a panel with the same geometry and build-up as tested in the in-situ experiments (presented in the previous section). The panel was supported along the top and bottom edges between strips of rubber. The impactor consisted of a steel weight encased in two tires and it was modelled as a 50 kg steel core covered in rubber with the geometry of the tires having a linear elastic material. Hexahedral solid-shell elements were used for the glass and interlayer parts while hexahedral solid elements with reduced integration were used for the rubber support parts. The global element size was 0.04 m while around the holes the size was 0.005 m. In total the number of elements was about 112 000. The glass, interlayer and supports were modelled as linear elastic materials with the material parameters adopted from Belis (2005), Persson and Doepker (2009), EN 572–2:2004 are shown in Tab. 1. The Young's modulus for PVB interlayer was calculated assuming the load duration in the range of 15-30 ms. The initial velocity of the impactor was set to 2.97 m s^{-1} which corresponds to a fall height of 450 mm. The full transient FE simulation of the panel and impactor were based on a previous model which is described in Fröling et al. (2014).

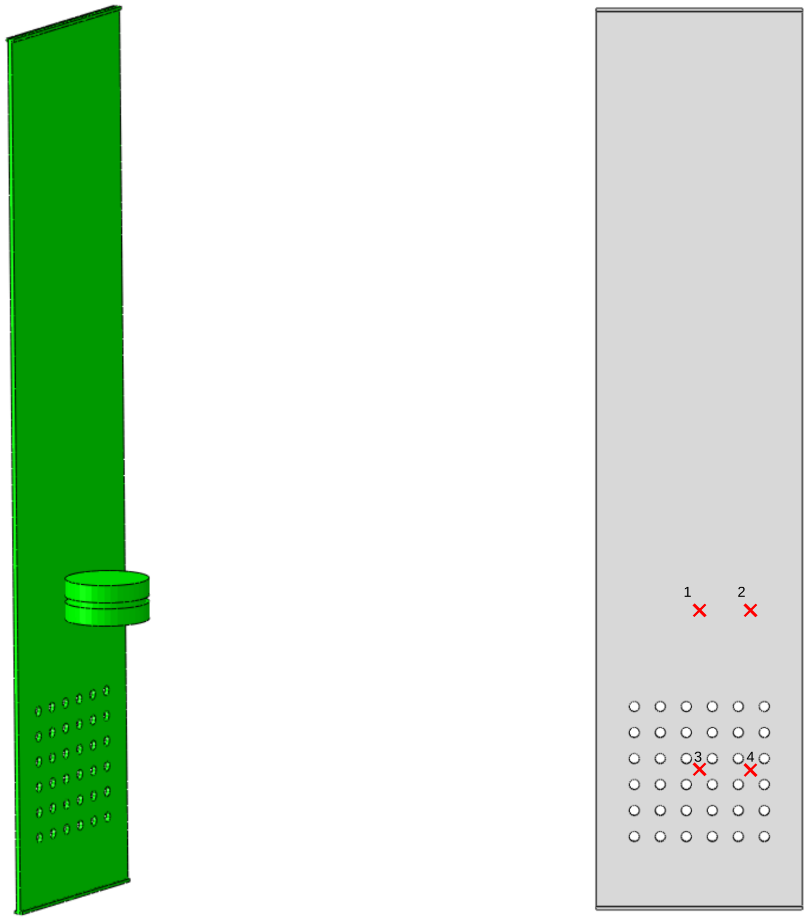

a) b)

Fig. 4 a) Tall panel and soft impactor. b) Selected impact locations.

Table 1: Material parameters (Belis (2005), Persson and Doepker (2009), EN 572–2:2004).

Material	E (MPa)	ν	ρ (kg m^{-3})
Glass	70 000	0.23	2 500
PVB interlayer	180	0.49	1 250
Rubber support	15	0.44	1 250
Impactor	2	0.30	900

Four impact locations were studied, two centerline cases at 600 mm and 1500 mm height, and two eccentrical cases 250 mm from the edge at 600 mm and 1500 mm height, respectively, see Fig. 4b. In addition, a panel with the same dimensions and material properties as before but without the array of holes was studied for the case of a centrical impact load at 1500 mm height. This was primarily made to study the influence of the holes.

In Fig. 5, the maximum principal tensile stress (MPTS) in the glass panel and the tensile stress at the impact location (on the opposite face of the panel) are shown for each of the four impact location cases. For cases 1 and 2, a second peak for the MPTS at 37 ms was found that corresponds to the stresses building up near the edges of the ventilation holes, in particular for the top row of holes. This causes the MPTS to increase by 40% as compared to the first peak corresponding to the tensile stress that is produced at the location of impact. In Fig. 6, the same data is shown in the case of the panel with the same dimensions but without the array of ventilation holes.

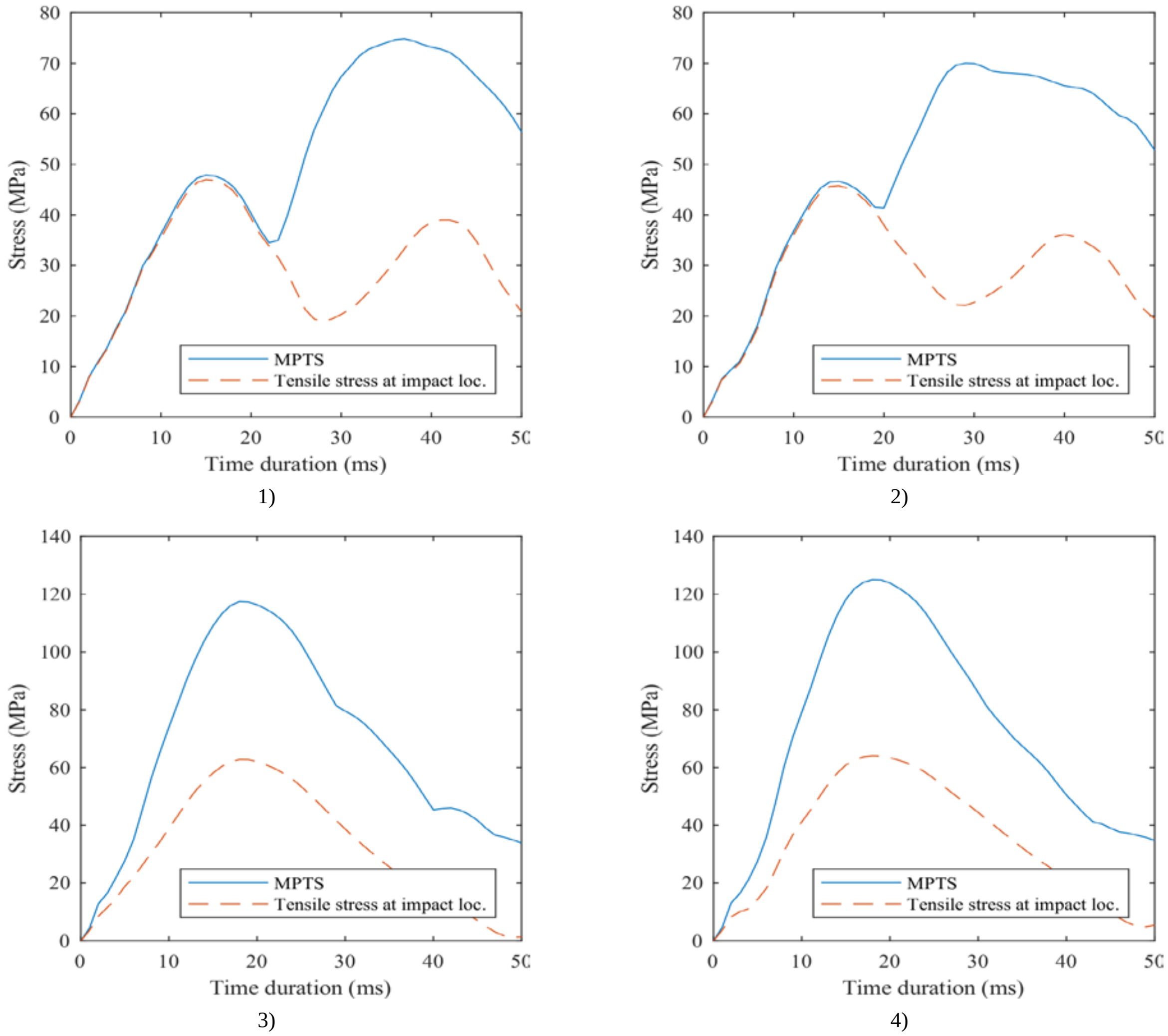

1) 2) 3) 4)

Fig. 5 Results of numerical simulations. Maximum principal tensile stress and tensile stress at the impact location (on opposite face of panel) in the four impact location cases.

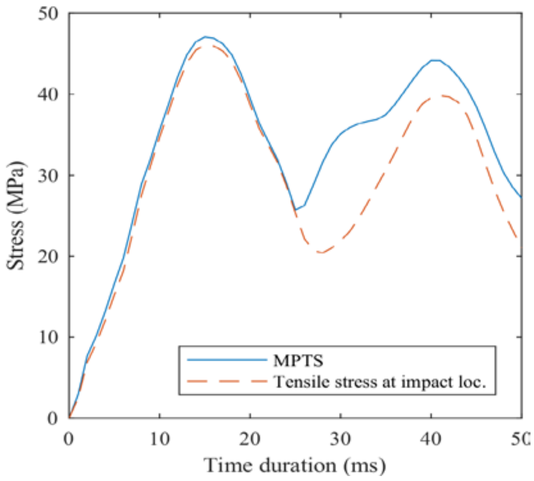

Fig. 6 Results of numerical simulations. Maximum principal tensile stress and tensile stress at the impact location (on opposite face of panel) in the case of the panel without an array of ventilation holes.

In Fig. 6, it is seen that by removing the ventilation holes from the FE analysis, the stress increase that was noted previously (Fig. 5, case 1 and 2), i.e. the second peak at time-duration 37 ms, is missing.

The maximum contact force is 11.8 kN and it is highest for the centric impact location at 1500 mm height, i.e. case 1. Fig. 7 illustrates the contact force time-history for case 1. The deflection rate at the impact location reaches about 1000 mm/s.

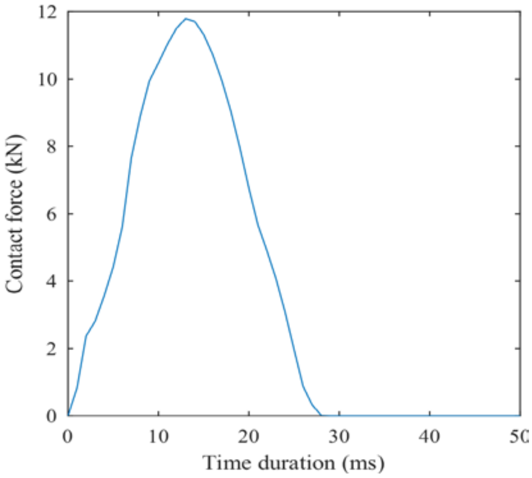

Fig. 7 Results of numerical simulations. Contact force time-history for impact location case 1.

Fig. 8 shows the maximum principal stress contours for the case 1 impact location at the two moments in time of 16 ms and 37 ms corresponding to the two peaks in Fig. 5a.

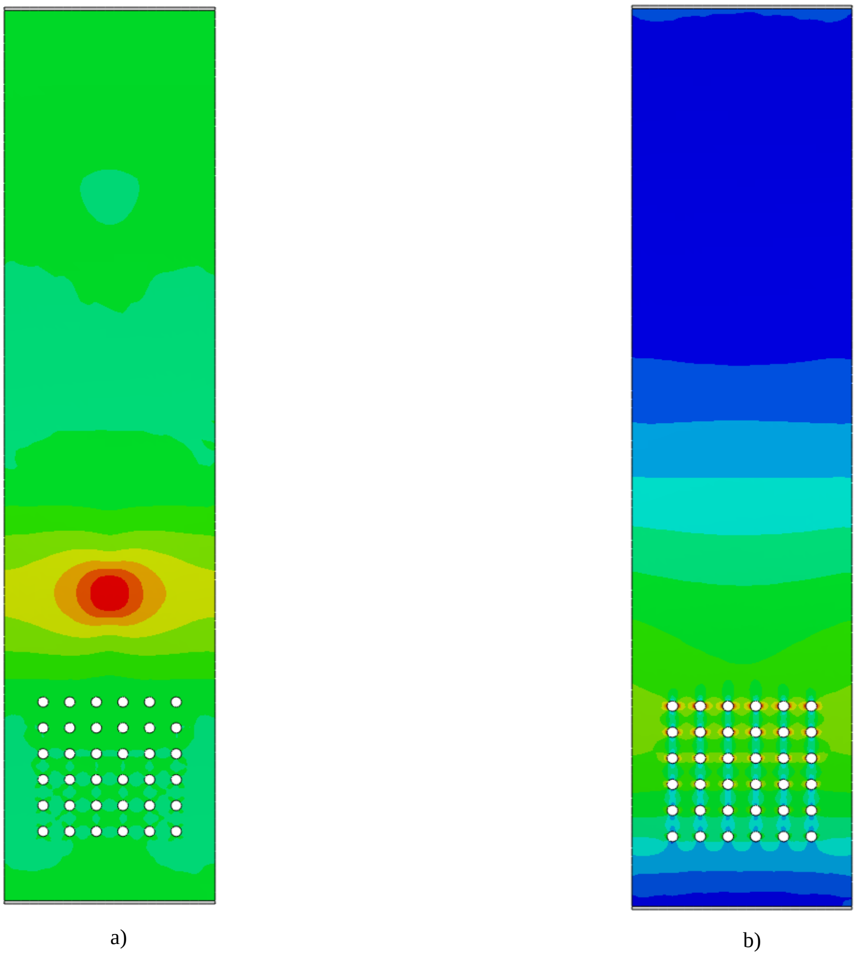

Fig. 8 Results of numerical simulations for case 1 impact location: a) Maximum in-plane principal stress contours at 16 ms and at b) 37 ms.

A simulation was carried out with the panel subjected to a static loading from the tires such that the contact force was equal to the maximum contact force during the dynamic impact case, see Fig. 7. Also, the location of loading was chosen in analogy with the impact location number 1, as detailed previously. The resulting distribution in maximum in-plane principal stress is shown in Fig. 9. It was found that the tensile stress around the holes was of approximately the same magnitude as the tensile stress at the load introduction point, i.e. about 95 MPa. Hence, a significant difference in stress distribution is noted between the static and dynamic load cases.

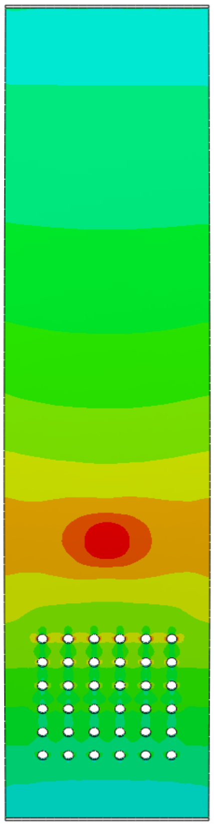

Fig. 9 Results of numerical simulations. Maximum principal stress contours in the case of static loading.

The impact location case 1 was investigated while substituting the interlayer material to Sentry Glass (SGP) by assuming a Young’s modulus of 500 MPa (instead of 180 MPa as previously when assuming PVB material). As can be seen in Fig. 10, the initial tensile stress response located at the impact location is reduced by about 10%, i.e. corresponding to the first peak in the diagram. However, the ultimate stress response located near the holes is still at the same magnitude as for the panel with PVB interlayer. This is due to the presence of stress concentrations around the edges of the holes which results in the stress of the same magnitude.

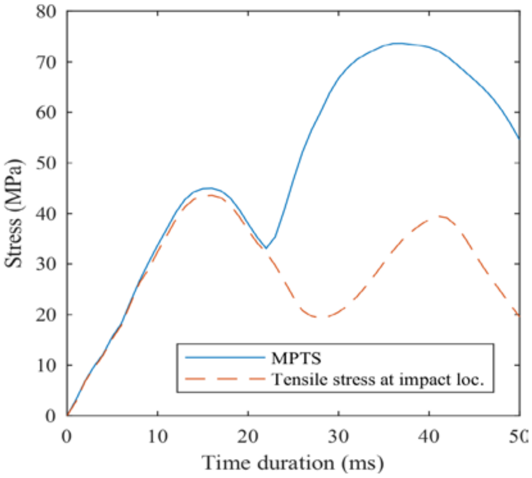

Fig. 10 Results of numerical simulations. Maximum principal tensile stress and tensile stress at the impact location (on opposite face of panel) in the case of SGP interlayer and assuming impact location 1.

4. Conclusions

This paper presents a structural analysis of slender glass panels widely used as storefronts and indoor separating walls in shopping malls and public buildings. It describes a case study of an indoor glass lantern in a public building made from slender two-side supported glass panels with a complex geometry and complementary numerical simulations.

The structural design of the panels presented in the case study was proven by experimental in-situ verification of the panels including static loading and soft body impact test. The results from the static loading test shows that under the loading of 1.0 kN/m, maximum stress and deflection is within acceptable limits. A clear influence on the stress by the holes was noticed. The stress around the edges of the holes was found to be approximately 40% higher compared to the stress at the introduction point of the jack. Keeping the constant load level for 15 minutes revealed approximately 40% decrease in stiffness of the panel which is mainly caused by stress relaxation of the viscous behavior of the interlayer. The soft body impact test proved the safety of the intact panel and the panel with one ply deliberately broken.

The numerical study showed that for a more complicated geometry, the stress distribution can dramatically change over time and that stress concentrations can develop at certain locations at a late stage in the impact history. In the study, a second stress peak in the load history was found due to the presence of the ventilation holes. The stress in glass increases by approximately 40% as compared to the first peak corresponding to the tensile stress that is produced at the location of the impact. The numerical study showed that the maximum contact force from the dynamic impact case applied to the panel as a static loading produces tensile stress of a higher magnitude. It was also found that the panel with the same geometry but with much stiffer interlayer material (SGP) exhibits an initial tensile stress response located at the impact location that is reduced by about 10%. However, the ultimate stress response located near the holes is still at the same magnitude as for the model with PVB interlayer.

References

Belis, J.: Kipsterkte van monolithische en gelamineerde glazen liggers. PhD thesis, Ghent University, 2005. (in English: Lateral-torsional buckling of monolithic and laminated glass beams).

Delincé, D., Callewaert, D., Belis, J.m Van Impe, R.: Post-breakage behaviour of laminated glass in structural applications. Proc. of the Challenging Glass conference on architectural and structural applications of glass, http://hdl.handle.net/1854/LU-416260, 459–467 (2008)

Fröling, M., Persson, K., Austrell, P.E.: A reduced model for the design of glass structures subjected to impact loads. Engineering Structures 80, 53-60 (2014)

Haldimann, M., Luible, A., Overend, M.: Structural Use of Glass, IABSE, Zürich (2008)

Persson, K., Doepker, B.: Glass panes subjected to dynamic impact loads. Proc. of the XXIV A.T.I.V. Conference, Parma, 9-10 July (2009)

Simulia. ABAQUS v. 6.14 computer software and online documentation, Dassault Systems, Providence, RI, USA, 2016

EN 572–2:2004. Glass in buildings - Basic soda lime silicate glass products. CEN, Brussels, Belgium.

EN 1991-1-1 Eurocode 1: Actions on structures - Part 1-1: General actions - Densities, self-weight, imposed loads for buildings. CEN, Brussels, Belgium.

EN 12600 Glass in building. Pendulum test. Impact test method and classification for flat glass. CEN, Brussels, Belgium.